Effect of Ionic Liquid Anion Type in the Performance of Solid Polymer Electrolytes Based on Poly(Vinylidene fluoride-trifluoroethylene)

R. Leones, [a,b] C. M. Costa, [c] A. V. Machado, [d] J. M. S. S. Esperança, [b] M. M. Silva, [a] and S. LancerosMéndez* Tc

Abstract

The effect of different anions within the ionic liquid in the characteristics of solid polymer electrolytes (SPEs) based on P(VDF-TrFE) has been investigated. 1-ethyl-3-methylimidazolium acetate, $[C_2mim][OAc]$, 1-ethyl-3-methylimidazolium triflate, $[C_2mim][(CF_3SO_3)]$, 1-ethyl-3-methylimidazolium lactate, $[\ C_2mim\ ][Lactate]$, 1-ethyl-3-methylimidazolium thiocyanate, $[C_2mim][SNC]$ and 1-ethyl-3-methylimidazolium hydrogen sulfate $[C_2mim][HSO_4]$ have been used in SPE prepared by sol-

Keywords: Battery separator membranes · Porous membranes · Ionic liquid · $P(VDF-TrFE)$

Introduction

Solid polymer electrolytes (SPEs) or ionic conductors are typically composed by a polymer with included salts, finding applications in the areas of batteries, sensors/actuators and supercapacitors, among others [1-3]. For battery applications, the salts are being replaced by ionic liquid (ILs), SPEs with ILs being a strong emerging class due to the improved safety and reliability of batteries [4]. The excellent properties of ILs include high ionic conductivity ($\sim 10^{-3} - 10^{-2}$ S cm^{-1}), almost null volatility, null flammability, thermal stability, wide electrochemical windows ($\sim 4 - 6$ V) and environmental friendliness [5].

The most relevant characteristics of ILs for tailoring specific properties to applications are density, viscosity, liquid range, vapor pressure, solubility, purity, electrical conductivity and electrochemical stability that depend on the cation and anion present in the ILs [6].

There are thousands of possible ILs available and the challenge is to determine which ILs are most appropriate and compatible with the polymer matrix used in a specific SPEs.

Fluorinated polymers, such as poly(vinylidene fluoride), PVDF, in SPE applications are very interesting due to their strong polarity (high dipolar moment) and high dielectric constant, showing also suitable mechanical and thermal properties. It is also possible to control the microstructure of the materials through binary and ternary polymer/solvent systems [7]. The inclusion of ILs within PVDF and its copolymers has not been enough investigated yet. The most used PVDF copolymers with ILs for SPEs applications are poly(vinylidene fluoride)-co-hexa-fluoropropylene, PVDF-HFP [8-11] and poly(vinylidene fluoride-co-trifluoroethylene), P (VDF-TrFE) [12].

The use of P (VDF-TrFE) as solid polymer electrolyte with (N,N,N-trimethyl- N-(2-hydroxyethyl)ammonium bis(trifluoromethylsulfonyl) imide, $[N_{111}(OH)][NTf_2]$ was demonstrated in [12], where the addition of the ILs affects the microstructure, thermal stability and ionic conductivity of the polymer membrane.

One interesting IL is 1-alkyl-3-methylimidazolium (C_nmim^+) and the influence of the alkyl-chain length n in its properties has been reported [13].

ILs based on 1- n-alkyl-3-methylimidazolium cation $[(C_nmim^+)][X^-]$, i.e., 1- n-butyl-3-methylimidazolium hexafluorophosphate $[C_4mim][PF_6]$; $1-n$-octyl-3-methylimidazolium hexafluorophosphate $[C_8mim][PF_6]$; $1-n$-decyl-3-methylimidazolium tetrafluoroborate $[C_{10}mim][BF_4]$ have been thus incorporated into membranes of PVDF [14]. The integrity and operational stability of the supported liquid membranes (SLMs) are not affected by the presence of the ILs.

There are also reports on the thermo-physical properties of ILs with anions, such as, $[BF_4]^-$[15], $[PF_6]^-$[16], $[Br]^-$[17], $[Cl]^-$[18] and $[EtSO_4]^-$[19], among others. For the same cation, 1-ethyl-3-methylimidazolium $[C_2mim]^+$, it is shown a complete database on the thermophysical properties of ionic liquids with different anions, including density, viscosity, refractive index, isobaric thermal expansivity and heat capacity of eight ionic liquids, allowing therefore the design of related industrial processes. Among the studied ionic liquids, [C_2mim] $[CH_3CO_2]$ is the best candidate for cellulose dissolution, showing also low viscosity and density-favorable properties for many industrial applications [20].

Taking into account the state of art of the thermophysical properties, viscosity and density, of the different anions and due to the interesting properties of the cation (C_2mim^+) and the P (VDF-TrFE) copolymer, this work investigates the effect of different anions within the IL for the development of SPE based on P(VDF-TrFE). 1-ethyl-3-methylimidazolium acetate, $[C_2mim][OAc]$, 1-ethyl-3methylimidazolium triflate, $[C_2mim][(CF_3SO_3)]$, 1-ethyl-3methylimidazolium lactate, $[C_2mim][$ Lactate $]$, 1-ethyl-3methylimidazolium thiocyanate, $[C_2mim][SNC]$ and 1-ethyl-3-methylimidazolium hydrogen sulfate [C_2mim] $[HSO_4]$ have been used for this purpose and the SPE were prepared by thermaly induced phase separation (TIPS). Polymer chain conformation, thermal and electrical properties are investigated as a function of the different anion present in the IL. These parameters are correlated with the density and viscosity for the different ILs. The understanding of effect of different anions within the polymer membranes allows the development and design of a novel generation by solid polymer electrolyte (SPEs) that can be used in energy storage applications.

Experimental

Materials

Poly(vinylidene fluoride-co-trifluoroethylene) (P(VDFTrFE)), (70/30), $Mw = 350000$ g/ mol, and the solvent $N,N-$ dimethylformamide (DMF, 99.5%) were obtained from Solvay and Merck, respectively.

The selected ionic liquids were 1-ethyl-3-methylimidazolium ethanoate, $[C_2mim][OAc]$, 1-ethyl-3-methylimidazolium trifluoromethanesulfonate, $[C_2mim][(CF_3SO_3)]$, 1-ethyl-3-methylimidazolium 2-hydroxypropanoate, $[\ C_2mim\ ][Lactate]$, 1-ethyl-3-methylimidazolium thiocyanate, $[C_2mim][SCN]$ and 1-ethyl-3-methylimidazolium hydrogen sulfate $[C_2mim][HSO_4]$. $[\ C_2mim][OAc]$, $[\ C_2mim]\ [HSO_4]$, $[C_2mim][(CF_3SO_3)]$ and $[C_2mim][SCN]$ were supplied by Iolitec with a stated purity of 95%, 99%, 99%

Table 1. Relevant properties of the different ionic liquids.

Ionic Liquid	Reference	$\rho(\mathrm{kgm^{-3}})$	$\eta(\mathrm{mPas})$
$[C_2\ \mathrm{mim}\ ][OAc]$	[20]	1099.3	143.61
$[C_2\ \mathrm{mim}\ ][(CF_3SO_3)]$	[20]	1385.9	42.936
$[C_2\ \mathrm{mim}\ ][\mathrm{Lactate}^2]$	[21]	1146.1	-
$[C_2\ \mathrm{mim}\ ][SCN^2]$	[20]	1117.0	24.505
$[C_2\ \mathrm{mim}\ ][HSO_4]$	[22]	1365.77	1628.4

and 98%, respectively. $[\ C_2mim\ ][Lactate]$ was supplied by Sigma Aldrich with a stated purity of 95%.

In order to reduce water and volatile compounds to negligible values, all samples were dried under vacuum (10^{-1} Pa) and vigorously stirred at moderate temperature (up to 330 K , depending on the anion) for at least a day. Coulometric Karl-Fischer titrations (Metrohm 831 KF Coulometer) revealed levels of water always below 300 ppm for $[C_2mim][HSO_4]$, $[C_2mim][(CF_3SO_3)]$ and $[C_2mim][SCN]$. For the more hydrophilic $[C_2mim][OAc]$ and $[\ C_2mim\ ][Lactate]$ the level of water was below 1500 ppm . This value is a conservative estimate that takes into account the uncertainty associated with the handling of the samples. Table 1 illustrates the chemical structure, density and viscosity of the different ionic liquids at $25°C$ and atmospheric pressure.

Solid Polymer Electrolyte Preparation

Solid polymer electrolytes were prepared by the solventcasting method. The host polymer P(VDF-TrFE) was dissolved at room temperature in N,N-dimethylformamide (DMF) (Merk, 99%) in a proportion of 15/85 and under magnetic stirring for a few minutes. Next, the respective IL was added in an IL/polymer weight ratio of 25% (w/ w).

The ILs content within the polymer membrane was chosen taking into account the compatibilization and miscibility between P(VDF-TrFE) and ILs. After complete dissolution, the solution was poured in a glass Petri dish within a gas

extraction chamber for 15 days in order to evaporate the DMF solvent at room temperature. Samples with an average thickness of 80μ m were obtained.

The polymer membrane without IL and the different polymer membranes with IL (different anions) will be called hereafter by pristine polymer, [OAc], [(CF_3SO_3)], [Lactate], [SCN] and [HSO 4].

Sample Characterization

Polymer phase and possible interaction between the IL and the polymer matrix were evaluated by Fourier Transformed Infrared Spectrostopy (FTIR) performed at room temperature with a Jasco FT/IR-4100. FTIR spectra were collected in the ATR mode from 4000 to 600 cm^{-1} after 32 scans with a resolution of 4 cm^{-1}.

The thermal behavior of the membranes was evaluated by differential scanning calorimetry (DSC) between 25 and 200°C, at a heating rate of $10°C min^{-1}$, under a flowing argon atmosphere, using a Mettler DSC 821e. Samples were transferred to 40μ L aluminum cans with perforated lids within a dry argon-filled glove box.

The degree of crystallinity (χ_c) was calculated (Equation 1) from the enthalpy of the melting peak (ΔH_f), taking into consideration the enthalpy of fully crystalline PVDF ($\Delta H_{100} = 103.4$ J/g) [23]:

$$\chi_c = \Delta H_f / \Delta H_{100} \quad (1)$$

Ionic conductivity and electrochemical stability were evaluated. Bulk conductivity of the electrolyte samples was obtained during heating cycles using the complex plane impedance technique on the cell GE/ polymer electrolyte/GE (GE stands for 10 mm diameter ion-blocking gold electrodes (Goodfellow, >99.95%)), secured in a constant volume support. Measurements were performed in a frequency range between 65 kHz and 500 mHz and a temperature range from 25 to 100°C using an Autolab PGSTAT-12 (Eco Chemie).

The ionic conductivity was calculated using Equation 2:

$$\sigma = d / R_b A \quad (2)$$

where σ is the ionic conductivity, R_b is the bulk resistance, d is the thickness and A is the area of the sample.

The evaluation of the electrochemical stability window of the electrolytes was carried out under an argon atmosphere at room temperature and within a Faraday cage using a two-electrode cell configuration: a 25μ m diameter gold microelectrode as working electrode and a lithium disk (cut from Aldrich, 99.9%; 19 mm diameter, 0.75 mm thick) as counter and reference electrodes. An Autolab PGSTAT-12 (Eco Chemie) apparatus was used to record voltammograms at different scan rates (0.05, 0.1, 0.5 and $1 Vs^{-1}$).

Results and Discussion

Morphological and Molecular Characteristics

Due to the used experimental procedure to produce the samples, the morphology of the SPE membranes is characterized by a porous microstructure similar to the one obtained for pure P (VDF-TrFE) and P (VDF-TrFE) with different IL contents of [$N_{1112}(OH)$][NTf_2] [12].

Figure 1a shows the free-standing solid electrolyte membranes with ILs.

All membranes are similar to the one shown in Figure 1a, exhibiting a white color independently of the anion present in the IL. The white color appearance (Figure 1a) is determined by the porosity of the polymer membranes obtained after the experimental procedure of solvent casting at room temperature [12]. The average

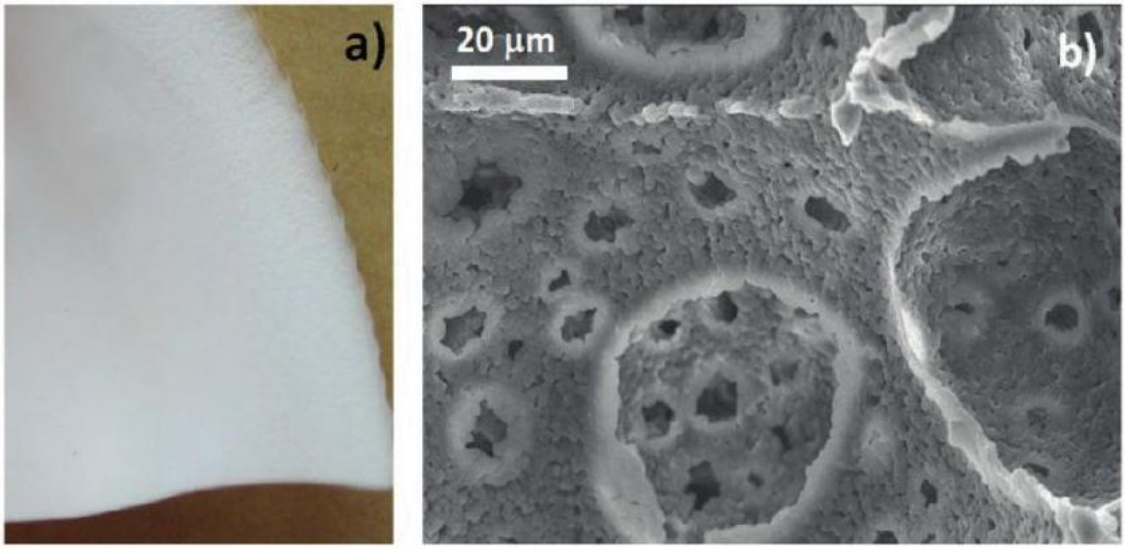

Fig. 1. a) Picture of the (CF3SO3) membrane, representative of the other ones, and b) porous microstructure characteristic of the membranes.
pore size and degree of porosity are ~ $9 \pm 3\mu$ m and 70%, independently of the IL [24], as shown in Figure 1b.
The porous microstructure of P (VDF-TrFE) is explained by the polymer/solvent phase diagram where a spinodal decomposition with liquid-liquid phase separation and crystallization of the copolymer rich phase occurs [25], together with the solvent evaporation.
Moreover, the physical stability of the polymer electrolyte membranes is not influenced by the inclusion of the IL within the polymer membrane structure in the sense that no fragmentation of the membranes is observed and mechanical integrity is maintained during sample handling.

Figure 2a shows the FTIR spectra for the pristine polymer and the SPEs with different ILs types in the region between 600 and 1800 cm^{-1}. In all cases the vibrational modes at 851 cm^{-1}, 886 cm^{-1} and 1402 cm^{-1} are observed [26], characteristics of the all-trans conformation of the polymer. This conformation is characteristic of the beta phase of the polymer, which is the polymer phase independently from the presence of the IL with the different anions.

The main effects of the IL in the FTIR spectra (Figure 2) are observed for $[(CF_3SO_3)]$ anion, which shows one vibration peak at 751 cm^{-1} that represents the symmetric deformation of the CF_3 portion of the CF_3SO_3 $^-$anions, $\delta_s(CF_3)$, assigned to ion-paired species [27]. Also for the same anion, it is detected at 1020 cm^{-1} one peak representing the symmetric stretching modes of SO_3 in the triflate anion.
The ion-polymer interactions can be also assessed from spectral changes in bands that consist primarily of molecular motions of the P (VDF-TrFE) polymer chains. For P (VDF-TrFE) polymer, one suitable region for evaluating ion-polymer interaction is the region of the $C-H$ stretching vibration between 2800 and 3300 cm^{-1} [28] (Figure 2b).

Figure 2b exhibits two peaks that represent the $P(VDF-TrFE)$ symmetric and asymmetric stretching vibrations of the CH_2 group at 2975 $cm^{-1}(\nu_s CH_2)$ and 3013 $cm^{-1}(\nu_a CH_2)$, independently of the anion type presents in ILs. It is also observed that the intensity of these peaks depends on the anion type. It has been reported

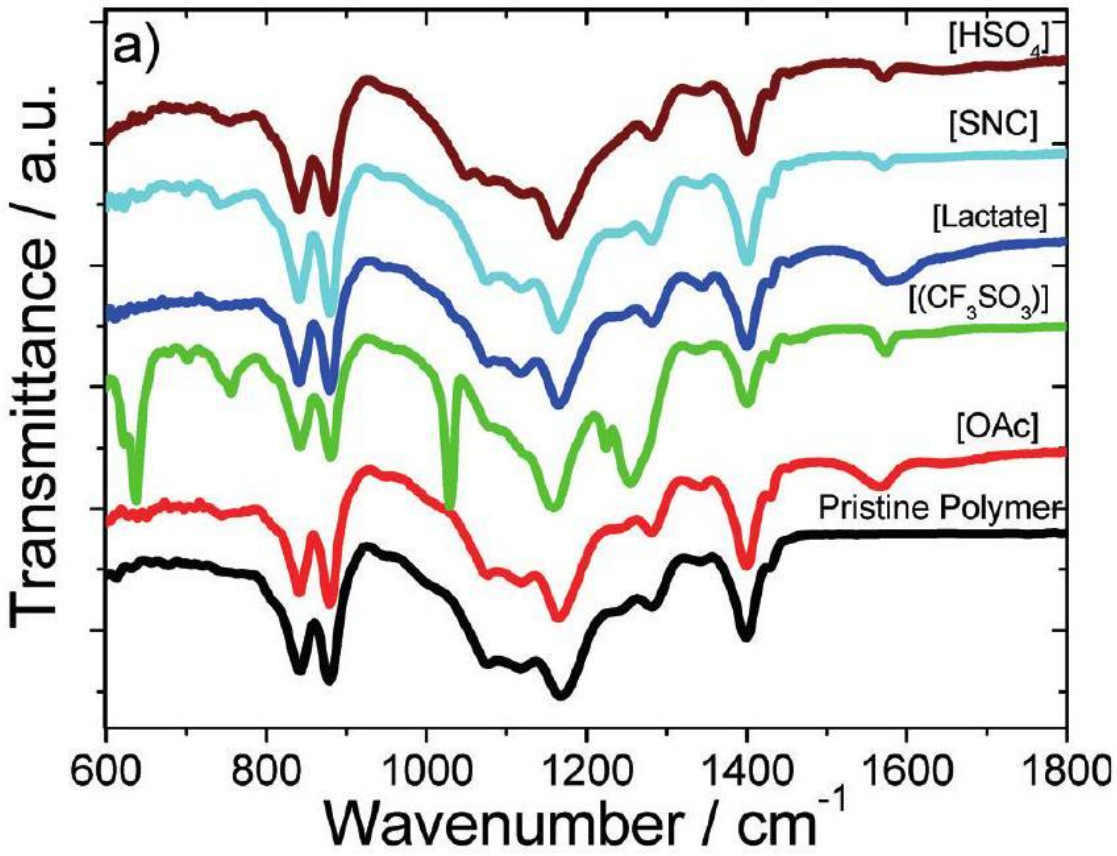
a)
[HSO4]
[SNC]
[Lactate]
[(CF3SO3)]
[OAc]
Pristine Polymer
Transmittance / a.u.
600
800
1000
1200
1400
1600
1800
Wavenumber / cm-1

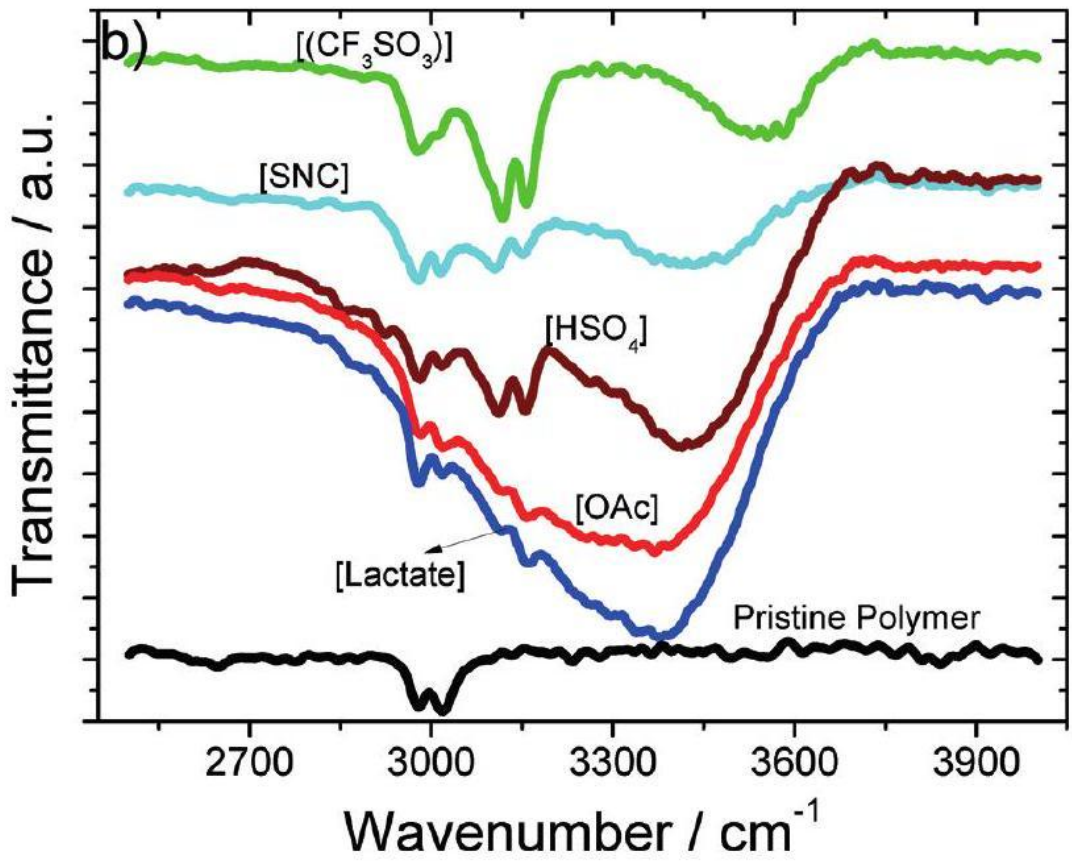
b)
[(CF3SO3)]
[SNC]
[HSO4]
[OAc]
[Lactate]
Pristine Polymer
Transmittance / a.u.
2700
3000
3300
3600
3900
Wavenumber / cm-1

Fig. 2. FTIR spectra of pristine P(VDF – TrFE) and the SPEs with different IL types: a) $600-1800\ cm^{-1}$ and b) the $C-H$ mode region at $2600-3900\ cm^{-1}$. for PVDF that the electrostatic interaction between the polymer chains and the ionic liquid becomes weaker for larger anions [29]. This fact is also observed in this work. In the region between 3150 at 3600 cm^{-1} multiple small bands are detected as well as one large band for all the SPEs, which is not present in the infrared spectrum of the pristine polymer. These bands prove the interaction between ion and polymers that depends on the anion size. For the large band, its intensity increases for the anions with larger size, i.e., [Lactate, $CH_3CH(OH)CO_2$] and [OAc, $(OOCCH_3)_4$)].

Thermal Properties

The DSC scans of the SPEs membranes are shown in Figure 3. The DSC scan of P(VDF-TrFE) is characterized by the presence of two endothermic peaks, the lower temperature peak corresponding to the ferroelectric-paraelectric phase transition (Curie temperature), identified by T_{FB} and the higher temperature peak representing the

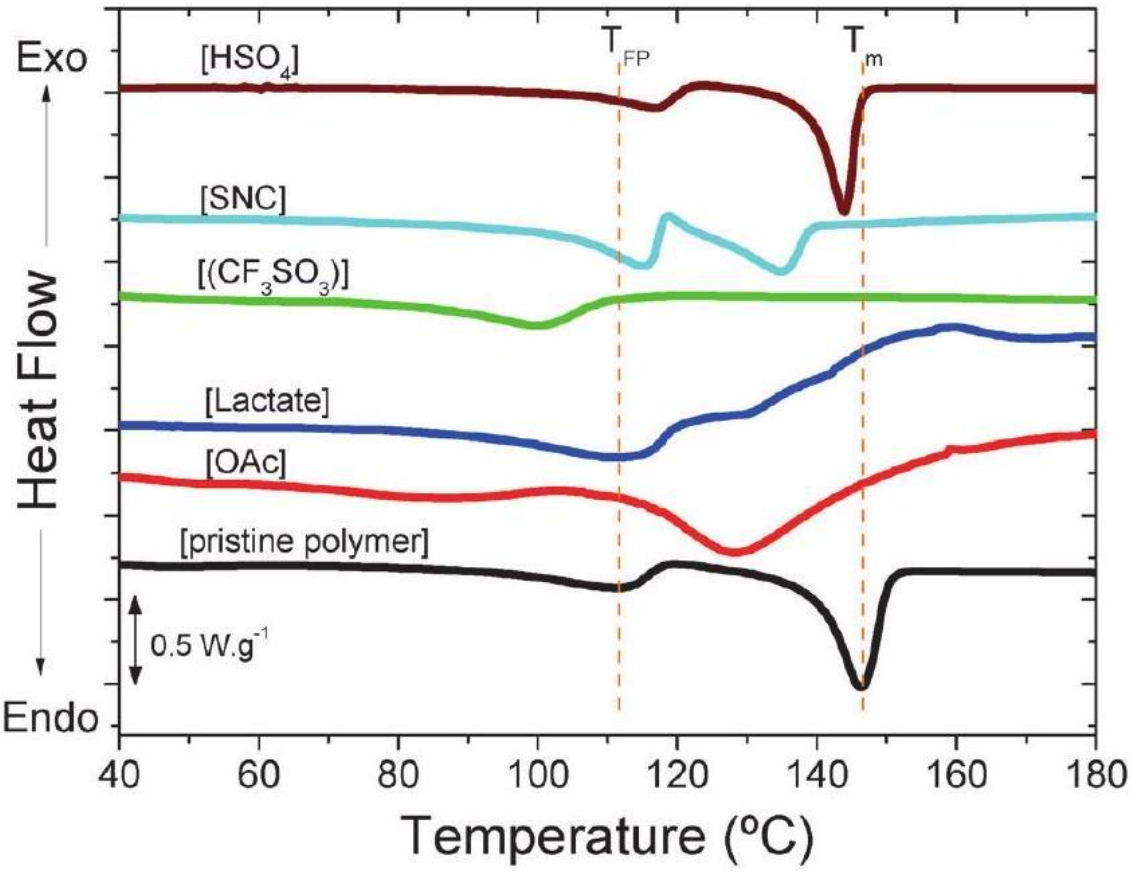

Fig. 3. DSC thermograms of the P(VDF – TrFE) membranes with ILs.

Table 2. Melting temperature (T_m), Curie temperature (TFP) and degree of crystallinity (χ_c) of the SPEs with different anion types, as determined from the DSC scans.

Samples	T_{PP} ($^\circ C \pm 2\%$)	T_m ($^\circ C \pm 2\%$)	χ_c ($\% \pm 2\%$)

Pristine Polymer	112	146	28
[OAc]	87	128	50
$[(CF_3SO_3)]$	-	100	18
[Lactate]	111	129	29
[SCN]	115	135	22
$[HSO_4]$	117	144	23

melting temperature, T_m. The temperature values for these peaks and the degree of crystallinity are shown in Table 2.

By comparing the DSC scans of the pristine polymer with the membranes with ILs, it is observed a shift for lower temperatures in both temperatures independently of the anion type. For all membranes, the melting temperature is between 146°C a 100°C and the Curie temperature between 112°C and 87°C (Table 2). Excepting for the [OAc] anion, the shift to lower temperatures of both transition temperature and melting temperature is related with a decrease in the degree of crystallinity. ILs can act as a directing agent to facilitate the crystallization process [30]. For high ILs content, these interactions may have a two-edged competitive effect on the crystallization: the promotion of polymer nucleation on the one hand and confinement effects on the other hand, leading to imperfections in the crystalline lamellas. The variation in the melting and Curie temperatures indicates miscibility and compatibility between polymer chains and IL.

For the [OAc] anion, the melting peak is more asymmetric and shows a larger area comparatively of the melting peak of the pristine polymer. The reasons for this fact are correlated to the thermal properties of [C_2mim]

[OAc]. The melting and decomposition temperature could not be determined for this ILs [31].

Electrical and Electrochemical Properties

The effect of the anion type of the ILs in the electrical properties was determined through electrochemical impedance spectroscopy. The Nyquist plot at 50°C is shown in Figure 4a for the different membranes. Typically, the Nyquist plot allows determining the mobility of ions due to charge transfer and diffusion processes. This plot show distinct parts: a semicircle located at the high-frequency range that corresponds to the charge transfer process and a straight line for lower frequencies that is related to the diffusion process [32,33].

Both processes are observed in Figure 4a independently of the anion type, i.e., the charge transfer and the diffusion process. For the [SNC] and [Lactate] anion types (Figure 4a), an overlapping semicircle is observed at high frequencies followed by a straight slanting line

at lowmedium frequencies.

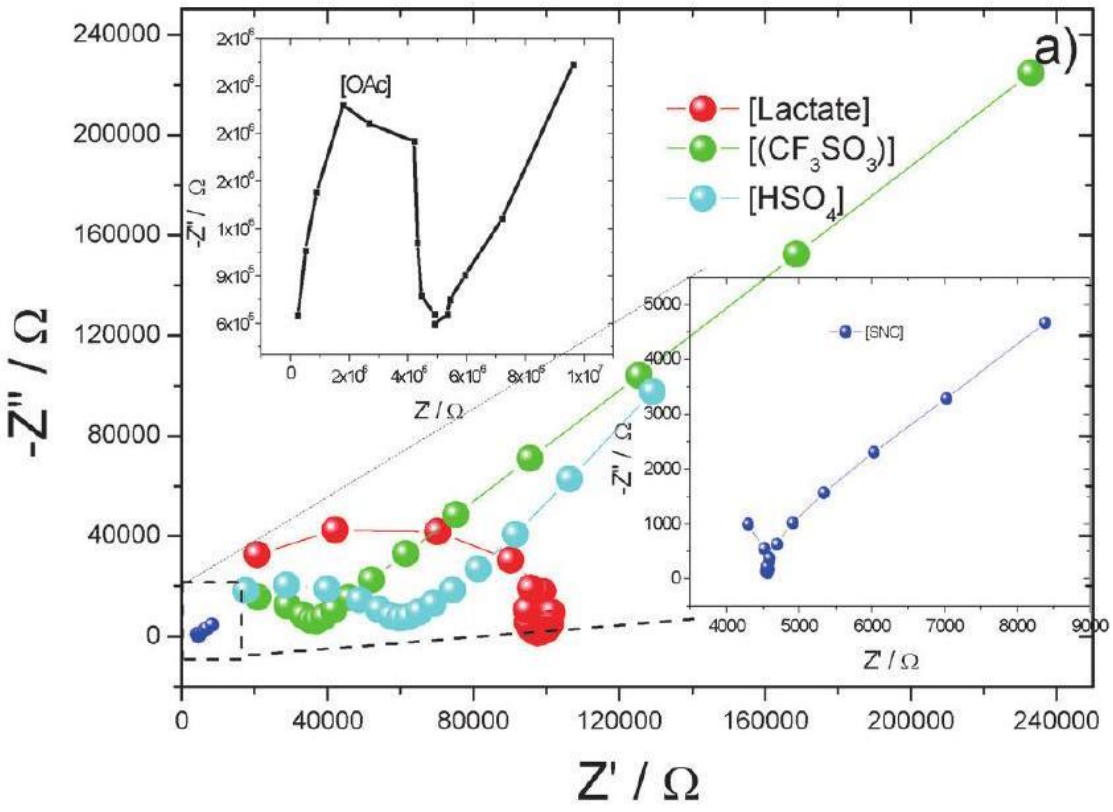
a)
[Lactate]
[(CF3SO3)]
[HSO4]
[OAc]
[SNC]
-Z'' / Ω
Z' / Ω
240000
200000
160000
120000
80000
40000
0
2x10^6
1x10^6
9x10^5
6x10^5
1x10^7
8x10^6
6x10^6
4x10^6
5000
4000
3000
2000
1000
9000
7000
6000

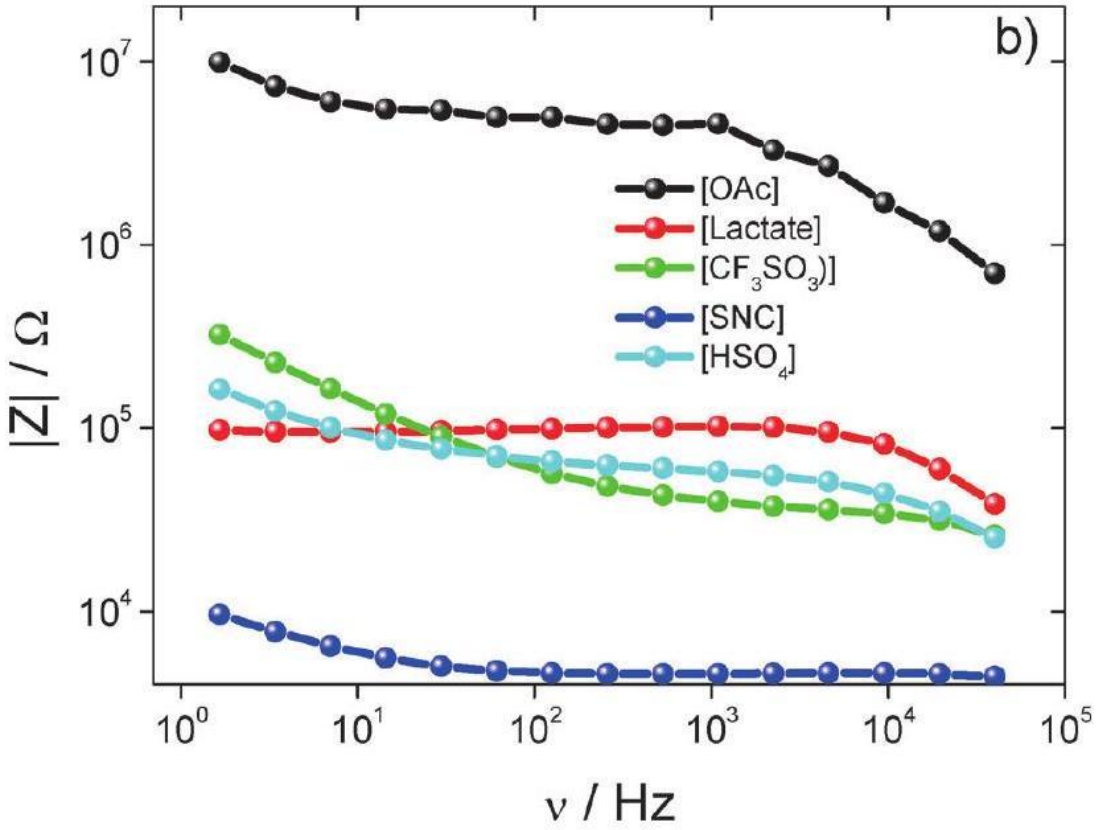
b)
[OAc]
[Lactate]
[(CF3SO3)]
[SNC]
[HSO4]
|Z| / Ω
ν / Hz
10^7
10^6
10^5
10^4
10^0
10^1
10^2
10^3
10^4
10^5

Fig. 4. a) Nyquist plot and b) impedance modulus as afunction of the frequency at 50°C for different SPE.

The inductive loop at high frequency is typically attributed to charge transfer across a double layer at the interfaces between the SPEs and the electrodes [34].

For ILs with different anion types the impedance modulus as a function of frequency is shown in Figure 4b. The impedance modulus decreases with increasing frequency for all samples and the impedance at 1 kHz follows the following trend: OAc > lactacte > HSO_4 > (CF_3SO_3) > SNC. This behavior, proportional to the value of the ionic conductivity, is related with the viscosity of the ILs. Independently of ILs type, the behavior of the impedance as a function of the frequency is ruled by the restricted dynamics of ion mobility within the porous membranes. The behavior of the phase angle as a function of frequency (not shows) is similar to the one of the impedance modulus.

Figure 5 shows the temperature dependence of the ionic conductivity of the SPE membranes. An increase of the ionic conductivity with temperature is interpreted as an ion hopping mechanism between coordinating sites together with local structural relaxations and segmental motions of the polymer salt complexes [35]. As temperature increases, the polymer chain acquires faster internal modes with bond rotations producing segmental motions. This, in turn, will favours inter-chain hopping and intrachain ion movements, which will increase the electrolyte conductivity [2,36]. Figure 5 also shows that the addition of any ILs produces an increase of the ionic conductivity with respect to the polymer matrix, mainly ascribed to the higher ionic charge content within the SPEs membranes. The highest room temperature ($T = 25°C$) conductivity for the electrolyte system is $0.002 mScm^{-1}$, obtained for the P(VDF-TrFE) based on [SCN]. At 100°C, this electrolyte exhibits a conductivity of $\sim 0.15 mScm^{-1}$. The differences in the conductivity values as a function of temperature of the samples with different ILs is related to the type of ILs, i.e., different anion type that affects

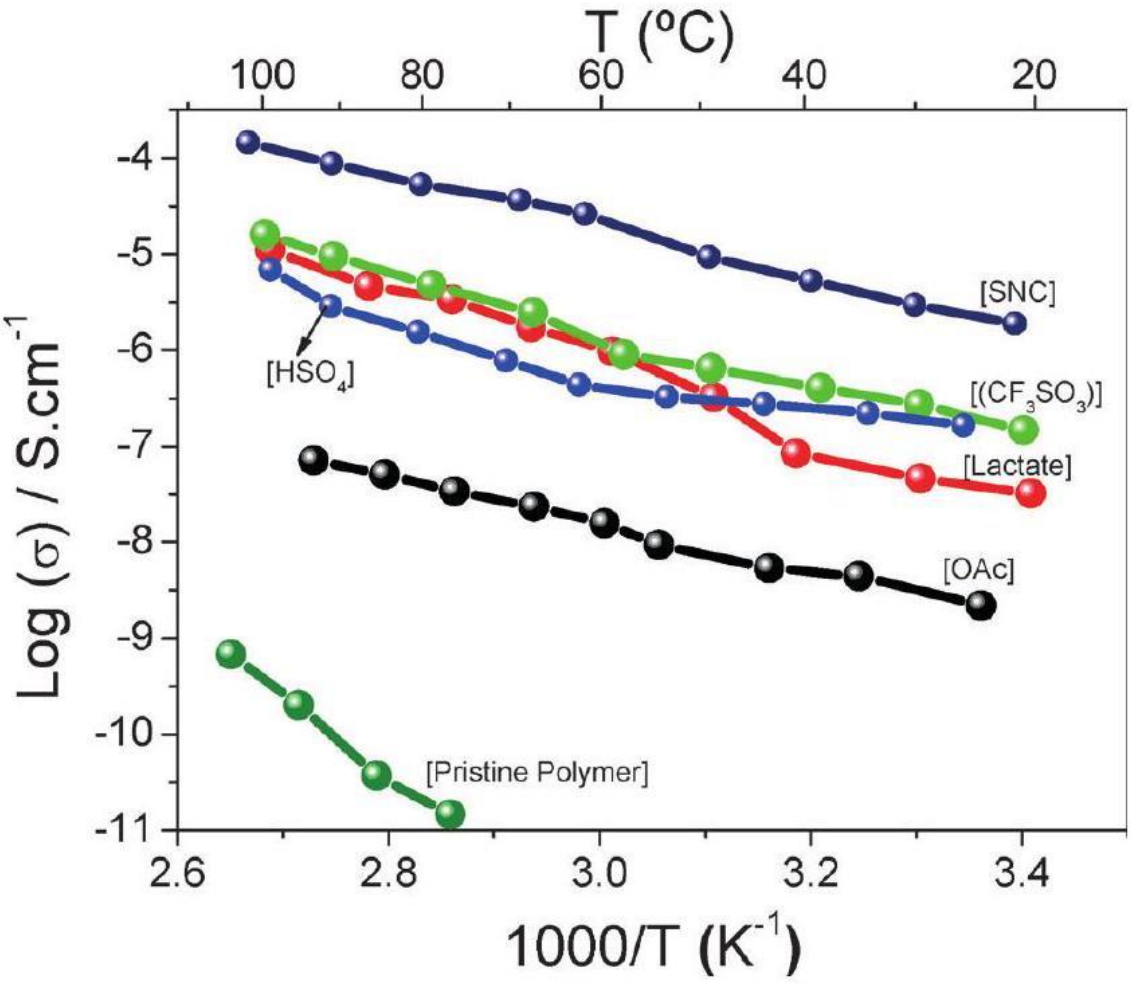

Fig. 5. Log σ as a function of $1000/T$ for the SPE membranes. the viscosity (Table 1) and the interaction between ILs and host polymer [37].

The temperature behavior of the ionic conductivity of the polymer electrolyte (Figure 5) membranes follows the Arrhenius equation in the measured temperature range:

$$\sigma = \sigma_0 \exp\left(-E_a/RT\right) \tag{3}$$

where σ is the ionic conductivity, σ_0, E_a, R and T are the pre-exponential factor, the apparent activation energy for ion transport, the gas constant (8.314 J/molK) and the temperature, respectively.

The obtained parameters after fitting the data from Figure 5 with Equation 3 are shown in Table 3.

The value of E_a for the electrolyte with [SCN] is 22.2KJmol^{-1}. This value is similar to the one reported for $P(VDF-TrFE)$ with 16wt% of $[N_{111}2(OH)][NTf_2]$[12] or other macromolecules [38]. The E_a values strongly decrease with the addition of ILs, which is related to the fact that the amount of ions in the polymer electrolyte increases, and the energy barrier to the ion transport decreases, leading to a decrease in the activation energy.

Comparing the conductivity data for different ILs within different polymers (i.e., PVDF, poly(ethylene oxide) (PEO), poly(vinyl alcohol) (PVA) and poly(methyl methacrylate) PMMA) [39,40], the developed materials show higher values. This could be explained by many factors: different purity of the ILs, different molecular masses of the polymer electrolytes based on ILs and the humidity of the atmosphere during the conductivity measurements. Schonhoff et al. [41] demonstrated that the conductivity of polymer electrolytes based on ILs depends on the humidity present during the measurement. The relevance of molecular mass and purity of the polymer electrolytes based on ILs on the ionic conductivity is shown in [37].

The viscosity of $[C_2mim][SCN]$ is 24.505 mPas , 42.936 mPas for $[\ C_2mim\ ]\ [CF_3SO_3]$ and 143.61 mPas for $[\ C_2mim\ ]$ [OAc], which may be related to the decrease in the magnitude of the positive charge of the imidazolium cation. The net force of attraction between the cation and anion decreases resulting in the diminution in the ionic character of $[C_2mim][SCN]$, which decreases viscosity [42,43]. The decrease in viscosity from 143.61 to 42.936 mPas and 24.505mPas(25°C) will lead to an increase in mobility which leads to increased conductivity. This fact is not observed for $[\ C_2mim\ ]\ [\ HSO_4\ ]$ polymer

Table 3. σ_0 and E_a for the SPEs as determined from the fitting of the data shown in Figure 5 with the Arrhenius equation.

Samples	$\sigma_0(\mathrm{Scm^{-1}})$	$E_a(\mathrm{kJ/mol})$
Pristine polymer	3.2×105	68.6
[OAc]	0.60	20.2
$[(CF_3SO_3)]$	15.2	23.6
[Lactate]	198.3	31.6
[SCN]	27.1	22.2
$[HSO_4]$	2.1	19.1

electrolytes as the viscosity is higher than for the others. Probably the reason is that for hydrogen sulfate based ILs, it is difficult to get below 1500 ppm of water. The influence of water on the conductivity was investigated in [43]. It was demonstrated that the lighter water molecules tend to displace much heavier counterions from the ion coordination shells, which reduce caging and increases the diffusivity, leading to higher conductivities.

The electrochemical window is an important parameter to be evaluated when application in electrochemical devices is intended. The electrochemical stability window of the P (VDF-TrFE)/IL membranes was determined by cyclic voltammetry (CV) over the -2.0 to 6.0 V potential at four different scan rates: 0.05,0.1,0.5 and 1.0 $\mathrm{V\ s^{-1}}$. In the CV plot the sweep potential was firstly scanned in the positive direction and then in the reversed direction (Figure 6). Figure 6a shows the good electrochemical stability of the [OAc] membrane. These voltammograms demonstrate that in the anodic region the sample is stable

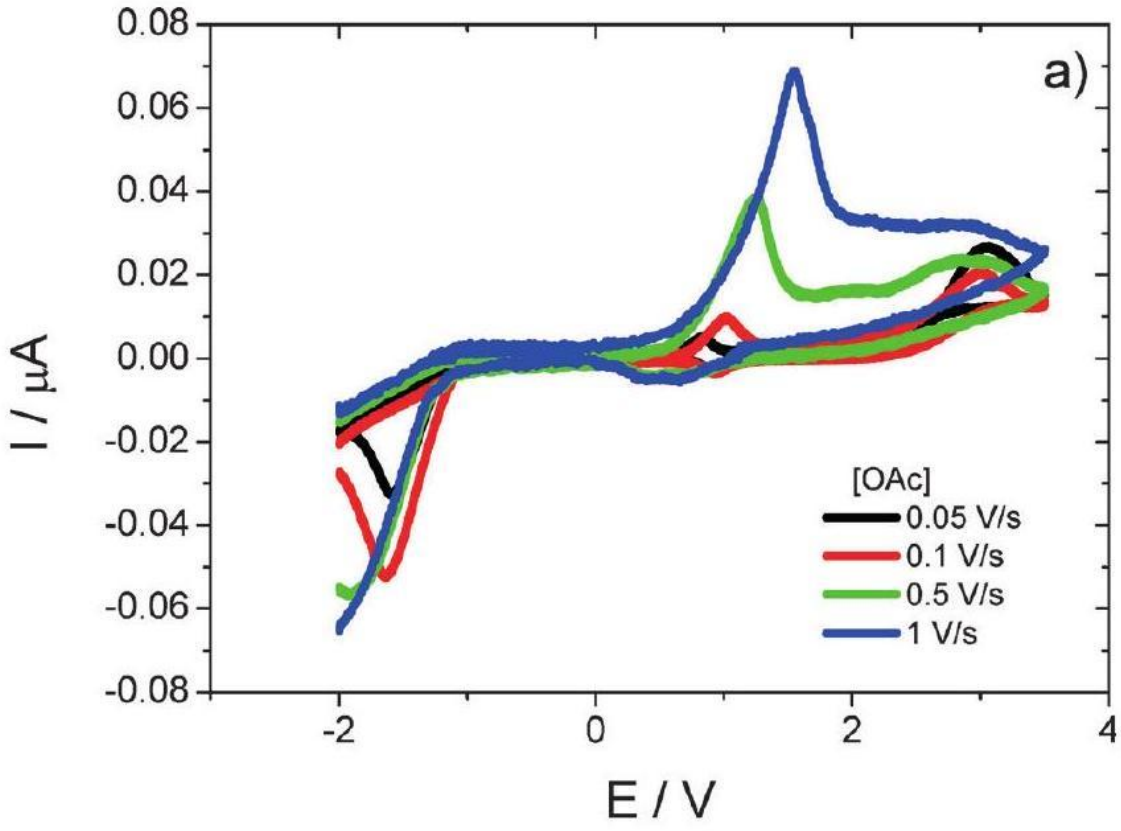
a)
0.08
0.06
0.04
0.02
0.00
-0.02
-0.04
-0.06
-0.08
I / µA
-2
0
2
4
E / V
[OAc]
0.05 V/s
0.1 V/s
0.5 V/s
1 V/s

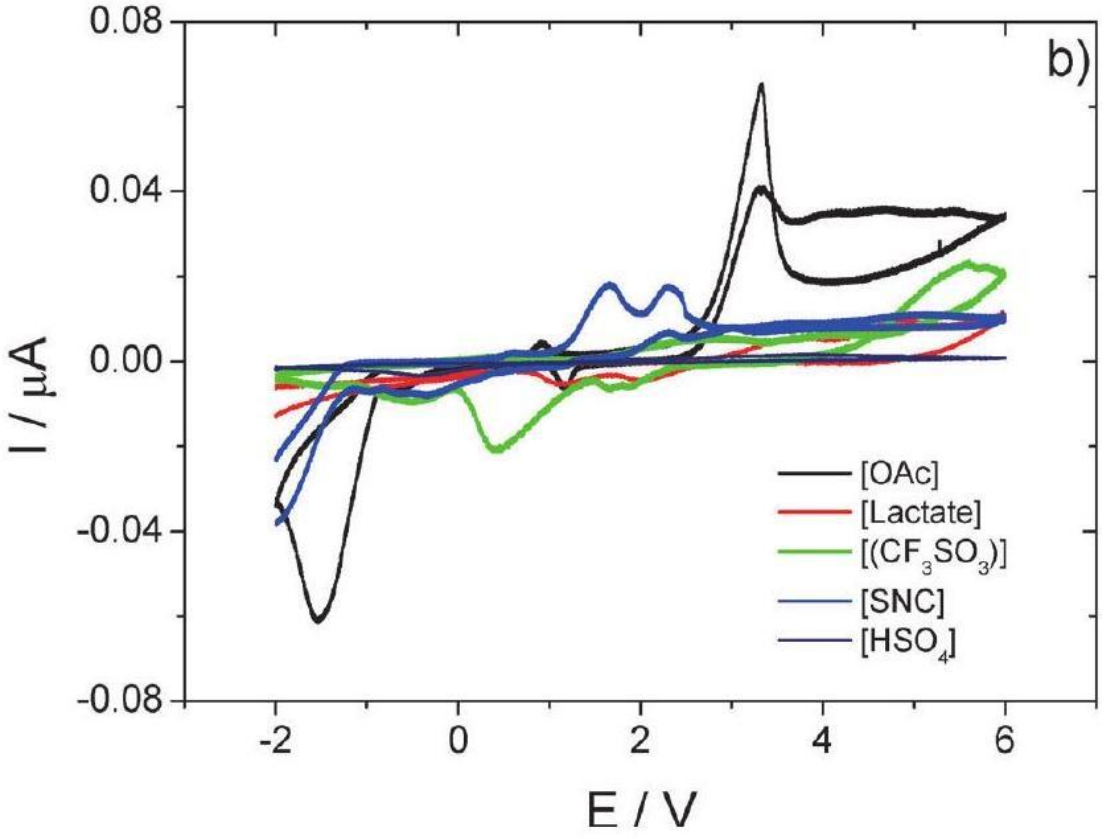
b)
0.08
0.04
0.00
-0.04
-0.08
I / µA
-2
0
2
4
6
E / V
[OAc]
[Lactate]
[(CF3SO3)]
[SNC]
[HSO4]

Fig. 6. a) Cyclic voltammogram of the [OAc] membrane at room temperature and different scan rates. b) The initial sweep direction is anodic and the sweep rate is 100mV/s for all samples.
up to about 0.8 V versus Li/Li^+, whereas in the cation region it is stable up to about -1.2 V versus Li/Li^+. The anodic current onset may be associated with the decomposition of the polymer electrolyte. This means that the overall redox stability of the [OAc] membrane spans about 2.0 V for high scan rates, an acceptable stability window for an application in a solid state electrochemical device. Figure 6a) also shows that increasing the scan rate leads to a shift into more cathodic and anodic peak potentials.

Figure 6b shows the cyclic voltammetry (CV) plots of the different SPE samples at a scan rate of 100mV/s in the potential window of -2.0 V at 6.0 V(vs. Li^2/Li^+). The apparent oxide and reduction peaks are detected for all samples except for [Lactate] and [HSO_4]. These peaks are observed in Figure 6b) depending on the anion type in the ILs. For [SNC] anion type, it is observed multiple anodic peaks.

Independently of the anion type present in the IL, the samples shown good electrochemical windows up to 3.0 V .

Conclusions

IL/P(VDF-TrFE) membranes were prepared by solvent casting with different ILs and the effect of varying anion type for a given cation was studied.

Independent of the anion type in the IL, the polymer matrix crystallizes in the polar phase. The interaction between the ILs and polymer depends on the anion size. The anion type also affects the degree of crystallinity and the melting temperature of the samples.

The ionic conductivity is higher for [SCN] anion type and its value depends on temperature. At room temperature, its value is $0.002 mScm^{-1}$ and for 100°C, the value is $0.15 mScm^{-1}$. Independently of the anion type, the ionic conductivity is more stable as a function of temperature when comparison with the sample without ILs.

The electrochemical stability evaluated by cyclic voltammetry revealed a stable operation window between -2.0 and 3.0 V , versus $Li/Li^+$for all samples.

The solid polymer electrolyte membranes presented in this work show adequate thermal, electrical and electrochemical properties for being used in specific applications.

Acknowledgements

This work was supported by FEDER through the COMPETE Program and by Fundação para a Ciência e Tecnologia (FCT) in the framework of the Strategic Project (PEst-C/QUI/UI0686/2014, PEst-OE/EQB/LA0004/2014, PEST-C/FIS/UI607/2014), project PTDC/CTM-NAN/ 121274/2010 and Grants SFRH/BD/68499/2010 (C. M. C.) and SRFH/BD/90366/2012 (R. L.). The authors thank funding from "Matepro-Optimizing Materialsand Processes", ref. NORTE-07-0124-FEDER-000037, co-funded by the "Programa Operacional Regional do Norte" (ON.2-O Novo Norte), under the "Quadro de Referência Estratégico Nacional" (QREN),

through the "Fundo Europeu de Desenvolvimento Regional" (FEDER). The authors thank Solvay for kindly supplying the high quality materials.

References

[1] D. T. Hallinan, N. P. Balsara, Annu. Rev. Mater. Res. 2013, 43, 503-525.
[2] F. M. Gray, Solid Polymer Electrolytes: Fundamentals and Technological Applications, Wiley, 1991.
[3] F. M. Gray, Polymer Electrolytes, Royal Society of Chemistry, Cambridge, UK 1997.
[4] B. Scrosati, J. Garche, J. Power Sources 2010, 195, 24192430.
[5] J. D. Holbrey, K. R. Seddon, Clean Products Proc. 1999, 1, 223-236.
[6] H. Ohno, Electrochemical Aspects of Ionic Liquids, Wiley, Chichester 2011.
[7] C. M. Costa, M. M. Silva, S. Lanceros-Mendez, RSC Adv. 2013, 3, 11404-11417.
[8] S.-H. Yeon, K.-S. Kim, S. Choi, J.-H. Cha, H. Lee, J. Phys. Chem. B 2005, 109, 17928-17935.
[9] S.-H. Yeon, K.-S. Kim, S. Choi, J.-H. Cha, H. Lee, J. Oh, B.B. Lee, Korean J. Chem. Eng. 2006, 23, 940-947.
[10] J. Fuller, A. C. Breda, R. T. Carlin, J. Electroanal. Chem. 1998, 459, 29-34.
[11] G. P. Pandey, S. A. Hashmi, J. Power Sources 2009, 187, 627-634.
[12] R. Leones, C. M. Costa, A. V. Machado, J. M. S. S. Esperança, M. M. Silva, S. Lanceros-Méndez, Solid State Ionics 2013, 253, 143-150.
[13] T. Shimomura, K. Fujii, T. Takamuku, PhysChemChemPhys 2010, 12, 12316-12324.
[14] R. Fortunato, C. A. M. Afonso, J. Benavente, E. RodriguezCastellón, J. G. Crespo, J. Membrane Sci. 2005, 256, 216223.
[15] K.-S. Kim, D. Demberelnyamba, B.-K. Shin, S.-H. Yeon, S. Choi, J.-H. Cha, H. Lee, C.-S. Lee, J.-J. Shim, Korean J. Chem. Eng. 2006, 23, 113-116.
[16] M. Sha, G. Wu, Q. Dou, Z. Tang, H. Fang, Langmuir 2010, 26, 12667-12672.
[17] A. Zare, A. Hasaninejad, A. Salimi Beni, A. R. MoosaviZare, M. Merajoddin, E. Kamali, M. Akbari-Seddigh, Z. Parsaee, Scientia Iranica 2011, 18, 433-438.
[18] A. C. Salvador, M. d. C. Santos, J. A. Saraiva, Green Chem. 2010, 12, 632-635.
[19] A. P. Fröba, H. Kremer, A. Leipertz, J. Phys. Chem. B 2008, 112, 12420-12430.
[20] M. G. Freire, A. R. R. Teles, M. A. A. Rocha, B. Schröder, C. M. S. S. Neves, P. J. Carvalho, D. V. Evtuguin, L. M. N. B. F. Santos, J. A. P. Coutinho, J. Chem. Eng. Data 2011, 56, 4813-4822.
[21] J.-Y. Wang, H.-C. Jiang, Y.-M. Liu, Y.-Q. Hu, J. Chem. Thermodyn. 2011, 43, 800-804.
[22] A. J. L. Costa, J. M. S. S. Esperança, I. M. Marrucho, L. S. P. N. Rebelo, J. Chem. Eng. Data 2011, 56, 3433-3441.
[23] R. S. Porter, J. Polymer Sci.: Polymer Lett. Ed. 1982, 20, 602-602.
[24] C. M. Costa, L. C. Rodrigues, V. Sencadas, M. M. Silva, J. G. Rocha, S. Lanceros-Méndez, J. Membrane Sci. 2012, 407408, 193-201.
[25] A. California, V. F. Cardoso, C. M. Costa, V. Sencadas, G. Botelho, J. L. Gómez-Ribelles, S. Lanceros-Mendez, Eur. Polymer J. 2011, 47, 2442-2450.
[26] A. A. Prabu, J. S. Lee, K. J. Kim, H. S. Lee, Vibrat. Spectrosc. 2006, 41, 1-13.
[27] C. M. Burba, ECS Transact. 2008, 13, 3-11.
[28] P. Martins, A. C. Lopes, S. Lanceros-Mendez, Progr. Polymer Sci. 2014, 39, 683-706.
[29] F. Wang, A. Lack, Z. Xie, P. Frübing, A. Taubert, R. Gerhard, Appl. Phys. Lett. 2012, 100, 062903.
[30] L. He, J. Sun, X. Wang, C. Wang, R. Song, Y. Hao, Polymer Int. 2013, 62, 638-646.
[31] J. Vitz, T. Erdmenger, C. Haensch, U. S. Schubert, Green Chem. 2009, 11, 417-424.

[32] B.-Y. Chang, S.-M. Park, Annu. Rev. Anal. Chem. 2010, 3, 207-229;
[33] M. Park, X. Zhang, M. Chung, G. B. Less, A. M. Sastry, J. Power Sources 2010, 195, 7904-7929.
[34] Q.-B. Zhang, Y.-X. Hua, J. Cent. South Univ. 2012, 19, 2451-2457.
[35] D. Baril, C. Michot, M. Armand, Solid State Ionics 1997, 94, 35-47.
[36] J. R. MacCallum, C. A. Vincent, Polymer Electrolyte Reviews, Springer, Heidelberg, 1987.
[37] A. S. Shaplov, E. I. Lozinskaya, D. O. Ponkratov, I. A. Malyshkina, F. Vidal, P.-H. Aubert, O. g. V. Okatova, G. M. Pavlov, L. I. Komarova, C. Wandrey, Y. S. Vygodskii, Electrochim. Acta 2011, 57, 74-90.
[38] J. Nunes-Pereira, A. C. Lopes, C. M. Costa, L. C. Rodrigues, M. M. Silva, S. Lanceros-Méndez, J. Electroanal. Chem. 2013, 689, 223-232.
[39] A. A. J. Torriero, M. J. A. Shiddiky, Electrochemical Properties and Applications of Ionic Liquids, Nova Science Publishers, Hauppauge, NY, 2011;
[40] Y.-S. Ye, J. Rick, B.-J. Hwang, J. Mater. Chem. A 2013, 1, 2719-2743.
[41] Y. Akgöl, C. Hofmann, Y. Karatas, C. Cramer, H.-D. Wiemhöfer, M. Schönhoff, J. Phys. Chem. B 2007, 111, 8532-8539.
[42] S. Tsuzuki, K. Hayamizu, S. Seki, J. Phys. Chem. B 2010, 114, 16329-16336.
[43] H. V. Spohr, G. N. Patey, J. Chem. Phys. 2010, 132, 234510.

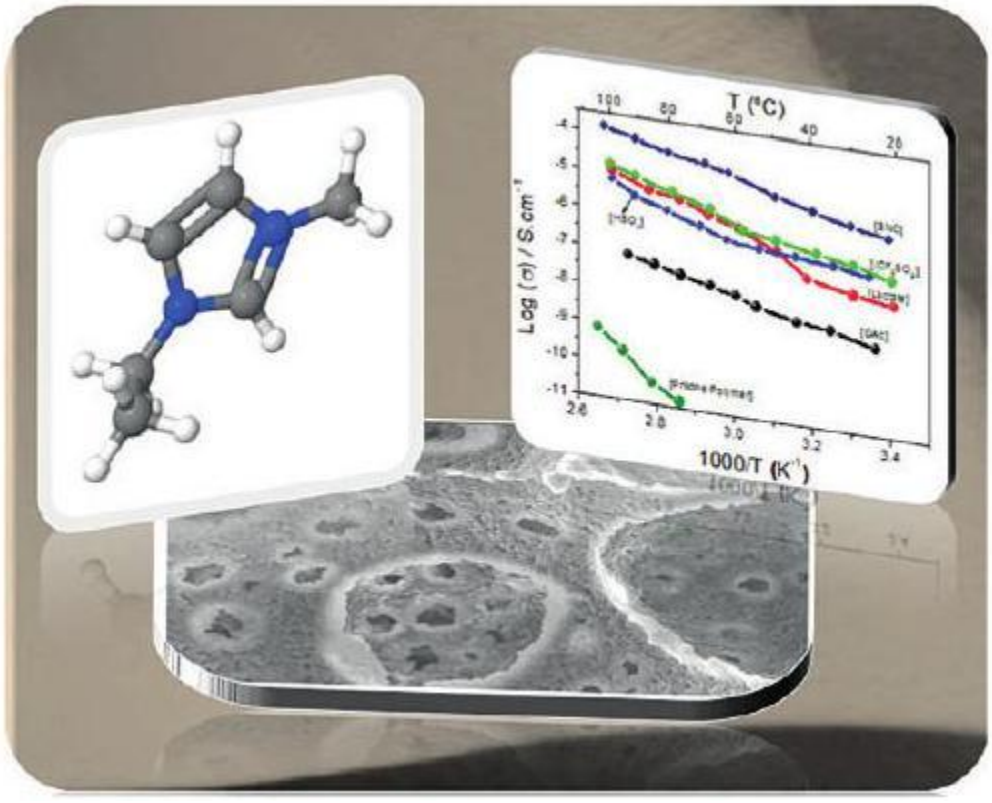

Effect of Ionic Liquid Anion Type in the Performance of Solid Polymer Electrolytes Based on Poly(Vinylidene fluoridetrifluoroethylene)